Astronomical Imaging with Infrared Array Detectors

Ian Gatley, D. L. DePoy, A. M. Fowler

History shows that progress in astronomy often stems directly from technological innovation and that each portion of the electromagnetic spectrum offers unique insights into the nature of the universe. Most recently, the widespread availability of infrared-sensitive two-dimensional array detectors has led to dramatic improvements in the capabilities of conventional ground-based observatories. The impact of this new technology on our understanding of a wide variety of phenomena is illustrated here by infrared pictures of star-forming regions, of nebulae produced by the late stages of stellar evolution, of the nucleus of our own galaxy (the Milky Way), and of activity in other galaxies.

In this century we have learned by experience that novel types of astronomical observation often lead to the discovery of new phenomena. We have, for example, witnessed the excitement that followed the inception of radio and x-ray astronomy and are no longer astonished by such concepts as that of neutrino astronomy. The fundamental importance of opening every conceivable observational window on our universe is widely appreciated.

One of the earliest demonstrations of this perspective was Sir William Herschel's well-known measurement of infrared radiation from the sun, made in 1800. Perhaps, then, it is surprising that infrared astronomy has not yet been fully exploited. This is especially true for those infrared wavelengths that penetrate through the earth's atmosphere, because they can be focused with existing "optical" telescopes. Yet no efficient way of imaging this infrared radiation existed until recently. Rather, because of the limitations on the existing technology and instrumentation, crude pictures were built up slowly and painfully using single detectors, by moving the telescope in a raster pattern.

To make images with single detectors is inefficient in obvious ways. Because the telescope must be pointed separately at each individual picture element, the procedure is inordinately time-consuming. Further, it limits the spatial accuracy of the image, discouraging work at high magnification and, since the data are taken serially, it maximizes susceptibility to variations in atmospheric conditions and instrumental performance.

Despite these difficulties, observations at infrared wavelengths are important because of several unique advantages. First, many cool objects (with temperatures less than about 1000 K) radiate predominantly in the infrared—these include, for example, low mass stars, planets, and clouds of circumstellar or interstellar dust. Second, infrared radiation penetrates through obscuring dust very much more easily than optical light; as we will see later, the center of our galaxy—the Milky Way—is undetectable in visible light, but is extremely bright in the infrared. Third, because of the cosmological redshift, the optical features of distant objects move to longer wavelengths. To compare the optical characteristics of very distant quasars and galaxies with their nearby counterparts, infrared measurements are required. (Although the term "infrared" is widely used to describe any wavelengths between 1 and 1000 μm, we will confine our attention here to results obtained in the wavelengths interval between 1 and 2.5 μm.)

Over the last two decades a community of dedicated astronomers has succeeded in demonstrating some of the virtues of infrared astronomy with primitive instruments, and, ever conscious of the potential advantages of even a modest camera, they have also vigorously pursued the possibility of technological innovations.

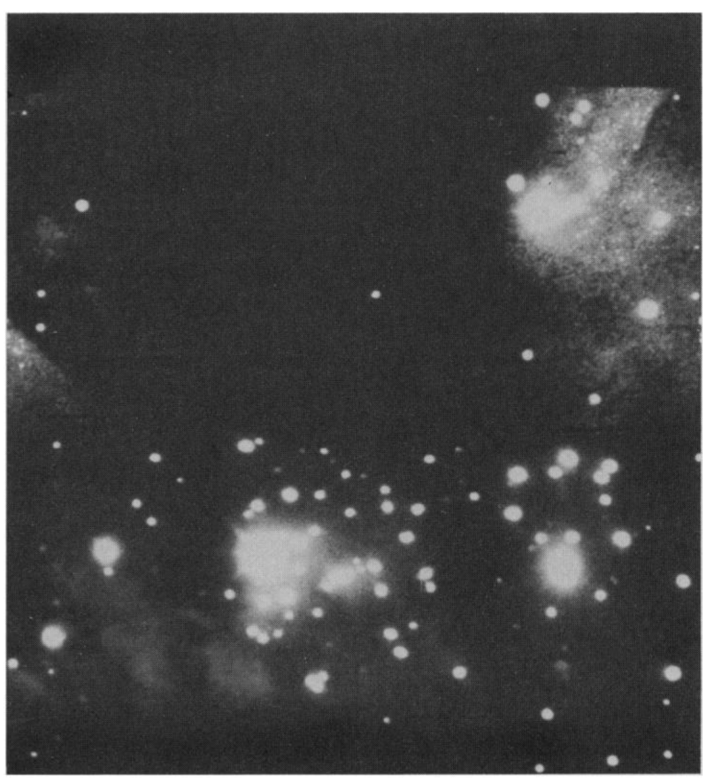

Fig. 1. Comparison of optical and infrared images of the star formation region NGC 2024 taken at (**top**) 0.7 μm, close to the red end of the visible range, and (**bottom**) 2.2 μm. The pictures were taken at the Kitt Peak National Observatory and are printed courtesy of R. Probst.

The authors are at the National Optical Astronomy Observatories, Tucson, AZ 85726.

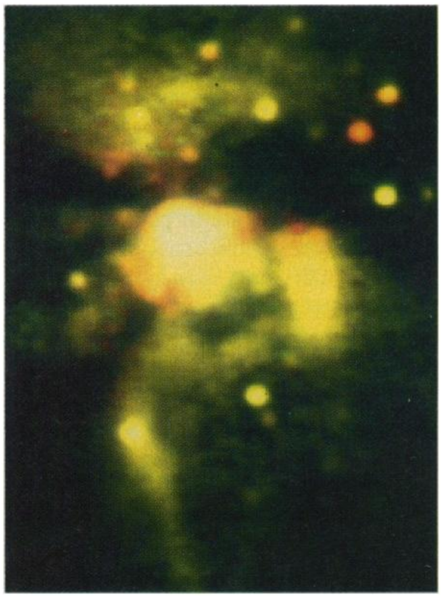

Fig. 2. An infrared image of Sharpless 106. The colors in the picture were produced similarly to the colors in the M17 picture on the cover. The picture was made with the University of Hawaii 2.24-m telescope at the Mauna Kea Observatory and is printed courtesy of K. Hodapp and E. Becklin.

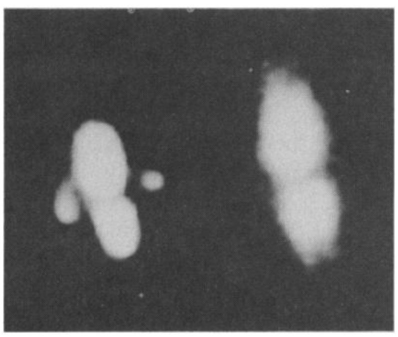

Fig. 3. Infrared pictures of CRL 2688 taken through (**right**) a wide bandpass filter centered on 1.25 μm and (**left**) a narrow bandpass filter centered on 2.122 μm, the wavelength of a strong molecular hydrogen emission line. No correction has been made for the continuum emission also present at this wavelength. As described in the text, a ring of emission appears at the "waistline." The images were made with the Kitt Peak National Observatory 1.3-m telescope in collaboration with B. Balick and B. Zuckerman.

Earlier this decade, encouragement came from the results of two camera projects, one at the NASA/Goddard Space Flight Center (*1*), the other at the University of Rochester (*2*), the former operating at wavelengths around 10 μm, and the latter from 1 to 5 μm. In both cases, despite the modest detector sensitivity, useful astronomical images were obtained.

Over the last few years major development efforts based on several different technologies, and often involving close collaboration between universities, industry, and government agencies, have gone ahead. By chance, many of these programs have achieved success simultaneously; in March 1987, at a remarkable meeting in Hawaii, a large number of exciting astronomical results obtained with two-dimensional infrared arrays were presented (*3*). Most of the detectors had been so recently commissioned that a telling bias emerged in the conference—the majority of the targets were in the wintertime sky!

The sudden impact on astronomy of sensitive two-dimensional arrays of infrared detectors—containing thousands of detectors, each more sensitive than the single detectors of earlier experiments—is the subject of this review. The changes in capability and perspective induced by this technological revolution are necessarily both profound and cumulative. We therefore feel the need to stress several points. First, the capability to make infrared images is suddenly rather widely available, and several viable technologies exist. Second, the pictures used to illustrate infrared imaging in the remainder of this review were obtained at a variety of observatories with these different technologies and many of the pictures have been kindly and enthusiastically provided by our colleagues. Third, it was difficult to decide which examples to choose and our choices were fairly arbitrary. Finally, it is our expectation and hope that these examples (and our descriptions of their astrophysical significance) will seem primitive when compared with the pictures that will be produced next year.

Star Formation Regions

How stars form is obviously of fundamental importance to astronomy. We know that massive stars form in clusters inside giant molecular clouds, but these clouds are dusty, and star formation is inefficient. Inevitably, then, the remnant cloud material obscures our view of star formation. Eventually the interactions between the massive young stars and the molecular cloud (such as stellar winds, whose effects are illustrated in the next section, and ionization of the gas by ultraviolet radiation) may disrupt the cloud sufficiently to render the stars detectable in optical light—the Orion Nebula is a familiar example.

To study the earliest phases of star formation, however, we must overcome the effects of obscuration. Infrared radiation penetrates through the dust; for example, if the dust attenuates the optical radiation by a factor of 1 million, then the infrared emission at 2 μm is attenuated only by a factor of 4.

Near the famous Horsehead Nebula in the obscured star-forming region NGC 2024 is the radio source Orion B. The radio emission in Orion B originates from a hydrogen plasma ionized by the ultraviolet radiation from the young stars. Fifteen years ago, infrared observations found a bright embedded star (*4*), but theory showed that this object was not sufficiently luminous to power the radio source alone (*5*). The generic problem of locating the members of young clusters embedded in their parent molecular cloud recurred in the study of star formation, simply because it was difficult to pursue such observational problems until infrared array detectors became available. Then, suddenly, it became trivial. We may compare images of the NGC 2024 region at wavelengths of 0.7 and 2.2 μm (Fig. 1). The dense dust lane that prevents us from detecting optical light from the young stellar cluster is penetrated in the 2.2-μm image. The nebulosity in the infrared image, like the radio emission, comes from the Orion B plasma.

On the cover of this issue is another example of star formation, the Omega Nebula (Messier 17). This spectacular nebula was discovered long ago by optical methods, but comparison of the optical and infrared images reveals that much of the source is heavily obscured by the dust in the molecular cloud. To illustrate the variations in the infrared colors throughout M17, three images were taken through infrared filters at wavelengths of 1.2, 1.65, and 2.2 μm; these three images have been displayed simultaneously in blue, green, and red, respectively. In other words, this is how M17 would look if the human eye responded to infrared rather than optical radiation, detecting wavelengths about three times longer than those of visible light. Some 80% of the hundreds of stars in this image were not detected before the advent of infrared imagers.

As in the case of Orion B, the nebulosity in M17 is plasma emission from hydrogen ionized by the radiation from the young stars. The variations in the apparent color of the nebula are caused by variations in the amount of foreground dust, as follows. We have already seen that longer wavelength radiation penetrates through the dust more readily; a corollary to this fact is that, as the amount of extinction by dust increases, the emergent radiation appears "redder." The optical picture of M17 is abruptly truncated at the right edge of the nebula, as the dust gets thicker; correspondingly, the infrared nebula appears systematically redder towards the right of

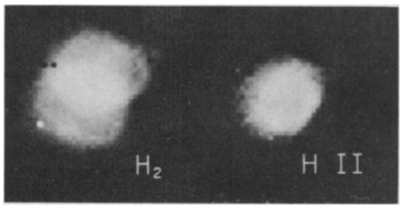

Fig. 4. A pair of infrared pictures of the planetary nebula NGC 7027 taken through filters which isolate radiation from molecular (**left**) and ionized atomic (**right**) hydrogen gas. The pictures were taken with the IRCAM instrument at the United Kingdom Infrared Telescope, Mauna Kea, Hawaii, courtesy of I. McLean.

the picture. It turns out that the most luminous part of M17 is totally invisible in optical photographs. The core of the M17 molecular cloud, one of the most massive in the galaxy, lies at the lower right of the region illustrated here (*6*); the total luminosity of the young stellar cluster is approximately 6 million times that of the sun (7).

A young star emerges from its parent cloud. Observations of radio molecular emission lines at millimeter wavelengths have shown that stellar winds from young massive stars are important in breaking up the "cocoon" of material left over from the collapse process that formed the star (*8*). The outflow of molecular material is often "bipolar," that is, it streams in two opposing directions. This bipolarity is probably related to the density structure in the "cocoon." In particular, any slight initial rotation of the parent molecular cloud prior to the cloud collapse will (after the huge scale change involved in the process, and because of conservation of angular momentum) cause the formation of a disk. The disk will collimate the stellar wind (in the direction perpendicular to the plane of the disk) and cause the bipolar flow.

An infrared image of Sharpless 106 (color-coded similarly to the earlier picture of M17), provides an example of a bipolar nebula viewed from a particularly favorable orientation, edge-on to the disk (Fig. 2). The young star is located in the disk, which separates the two lobes. The dust in the disk is responsible for the red color of the nebula at the edges of the disk and the red or orange color of background stars shining through the disk, which plainly suffer substantial amounts of extinction and reddening.

Planetary Nebulae: Late Stages of Stellar Evolution

The final stages of stellar evolution often involve the loss of material from the star, and the formation of circumstellar nebulae. When the mass loss is extreme, there is enough material in these nebulae to extinguish the optical light from the star. It is straightforward to see the importance of infrared observations in such cases. Less highly obscured mass-loss nebulae, including the famous and often photographed "planetary nebulae" (of which the Ring and the Dumbbell nebulae are well-known examples) are also good targets for infrared cameras. The reason is that a critical observational strategy is uniquely available in the infrared, namely, to observe emission lines from the hydrogen molecules. [Although we will illustrate molecular hydrogen imaging only for the case of planetary nebulae, the technique can be applied in many circumstances. One may confidently predict that it will be widely used, and with important consequences (*9*). Indeed one might have expected that observations of molecular hydrogen, which is astrophysically the most abundant molecule by an overwhelming factor, would dominate the field of molecular line astronomy. The hydrogen molecule, however, is homonuclear—and so lacks a dipole moment—which implies immediately that its emission lines will be weak compared to those of many other (less abundant) molecules; furthermore it is difficult to excite. Suffering neither disadvantage, the CO molecule has been widely observed in astronomy. The hydrogen molecule is excited in astrophysical shocks with velocities in the approximate range 10 to 50 km/s, and by ultraviolet light in the wavelength interval 912 to 1108 Å (*10*); the electric quadrupole transitions of its vibration-rotation spectrum can be observed in the infrared.]

As it happens, both molecular hydrogen excitation mechanisms may plausibly operate in planetary nebulae, because the mass loss wind from the central star can shock the envelope, and ultraviolet radiation sufficient even to ionize portions of the envelope is emitted from the stellar remnant. Fortunately the relative strengths of the emission lines resulting from the two excitation mechanisms are very different, and so we can distinguish between them.

The ionized gas in planetary nebulae is easy to detect, and has been studied in detail, but detection of the neutral component presents more of a technical challenge. We need to know the distribution of the neutral gas in order to attack a fundamental unsolved question, namely, that of the physical mechanism that ejects and shapes the outflowing envelope. An interesting form of planetary nebulae, the "bowtie" or "butterfly"—typified by the Dumbbell nebula (Messier 27)—commonly shows molecular hydrogen emission (*11*). We have observed a dense molecular toroid around the "waistline" of several of these objects; Fig. 3 is an image of a nebula known as CRL2688 (the toroid appears in projection as two circular patches at the waistline). The morphological similarity between this bipolar nebula and the young object Sharpless 106 is striking; the appearance of each is dictated by the presence of a dense disk that collimates an outflow.

CRL2688 was easily identified as a bipolar nebula from optical observations. Another planetary nebula, NGC 7027, exhibits no hint of bipolarity in optical or radio data (Fig. 4). The ionized gas distribution, labeled H II (imaged here in the $n = 7 \rightarrow 4$ recombination line of atomic hydrogen at 2.17 μm), forms a bright oval shell. In sharp contrast, the molecular hydrogen image exhibits a bipolar structure and a dense toroid.

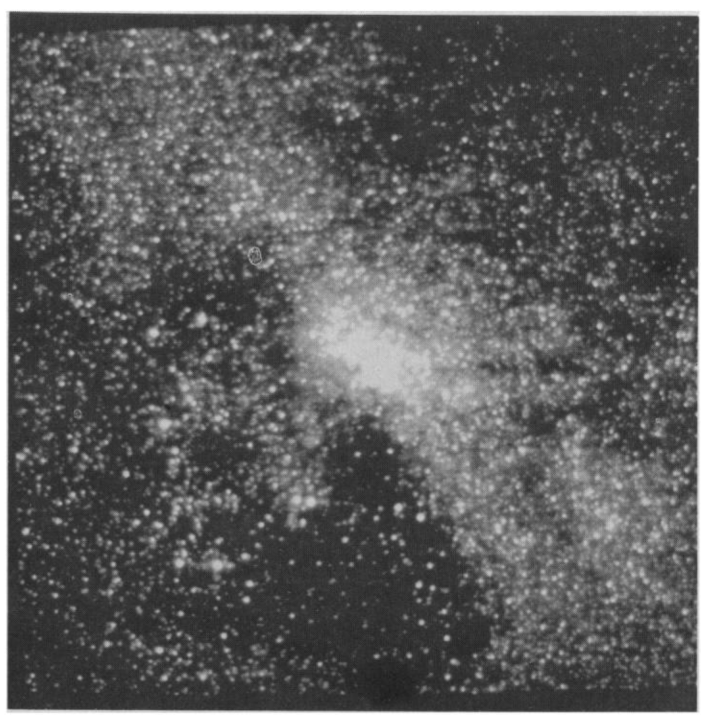

Fig. 5. A 2.2-μm infrared picture of our galactic center taken with the Kitt Peak National Observatory 1.3-m telescope.

The Center of Our Galaxy

The nuclei of galaxies are regions of high stellar density that often exhibit remarkably energetic activity. The energy density is sometimes so high that the only "conventional" physical explanation available is that of emission from the accretion disk of a black hole. The nucleus of our own galaxy—the Milky Way—is some 100 times closer than even the nearest neighboring spiral galaxy, Andromeda. This simple fact provides us with a compelling motivation to study the galactic center, for we are guaranteed to obtain detailed information unavailable to us elsewhere; but, there is a problem. The outer part of our galaxy is an enormous, flattened, very dusty disk (exactly like that seen in many familiar pictures of distant galaxies). We live out in the disk. Optical astronomers cannot, therefore, exploit our proximity to the nucleus, because the intervening dust obscures optical radiation.

The position of the nucleus was determined by infrared observations in 1968 (*12*), and a large body of information has been painstakingly accumulated since then by infrared and radio observers, as described, for example, in the recent symposium to honor Charles Townes (*13*). Considerable effort and ingenuity have been expended in the pursuit of observational data and in their interpretation. There is evidence for significant nuclear activity, corresponding to an energy output some 10 million times that of the sun. There has been lively discussion of the implications of this result, which may be attributable to star formation, or may perhaps be emission from the accretion disk of a black hole. Useful tests of the various hypotheses are provided, for example, by the study of the stellar population, by measurements of the radial distribution of starlight, and by determination of the kinematics of the stars and the gas.

The impact of infrared cameras on this field is enormous. A striking instance is Fig. 5, which was obtained in less than 1 hour on a 50-inch (1.3-m) telescope, and which shows a 2.2-μm image of the central 100 light-years of our galaxy. The nucleus is prominent at the center. Thousands of stars are detected, and the direction of the plane of the galaxy, which runs from upper left to lower right, is evident. A large patch of extinction runs parallel to the plane, displaced down to the left; this is caused by dust in the galactic plane. One may immediately deduce that our vantage point (that is, the solar system) is actually slightly displaced above the plane of the galaxy.

More importantly, this image provides some perspective on the practical issues involved in the studies of the galactic center, and vividly demonstrates how vast a strategic problem confronted the observer using a single detector. It would have been necessary to point the telescope at half a million positions on the sky in order to build up a picture like Fig. 5. The reward for such a heroic effort would have been to confront head-on the question of which of these thousands of stars needed to be studied in more detail; and, remember, they would need to be studied one at a time!

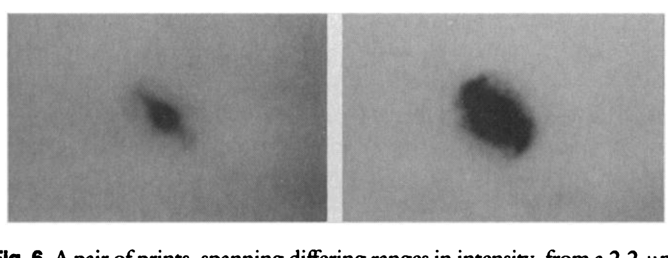

Fig. 6. A pair of prints, spanning differing ranges in intensity, from a 2.2-μm infrared image of NGC 1068 taken with the ARC camera (constructed at the Yerkes Observatory of the University of Chicago) at the University of Wyoming Infrared Observatory 2.3-m telescope, courtesy of H. Thronson, M. Hereld, and A. Harper. (**Left**) Shows the central bar and the compact bright nucleus. (**Right**) Including a wider range in intensities, shows the spiral structure of the galaxy.

Virtually every experiment performed before arrays, then, was necessarily based on preconceived ideas about the problem. The new detectors remove this bias. Discoveries generally follow swiftly in such circumstances. The first round of activity will naturally be to improve our determination of those physical quantities relied upon most heavily in current analyses: the types of stars present, the extinction they suffer from intervening dust, and their distribution in space; the excitation of the ionized and molecular gas; the dynamics of the gas and stars. All this, and more, while diligently searching for anomalies suggestive of a black hole.

Activity in Other Galaxies

In other galaxies both the amount of star formation activity and the luminosity of the nucleus is sometimes far in excess of that in our galaxy. This is demonstrable from optical observations alone, but we can confidently anticipate (from consideration of the infrared pictures of our own galaxy) that infrared pictures of other galaxies will provide new insights.

For example, the galaxy NGC 1068 has a bright nucleus surrounded by a very luminous star-forming region some 10,000 light-years in diameter (*14*). Speculation about the relationship, if any, between the compact nuclear source and the extended star-forming region has abounded. Accretion of material onto the nucleus, or the triggering of star formation by an explosion in the nucleus, are popular scenarios. The discovery, made by the Infrared Astronomy Satellite (IRAS) satellite (*15*), of a possible correlation between nuclear luminosity and the presence of stellar bars (*16*) led to suggestions that barlike structures are important in radial transport of material, but optical observations failed to reveal a bar in NGC 1068. The optical observations may, of course, have been hampered by dust, and are also strongly biased by the bright emission from the recently formed stars. Infrared observations, besides penetrating the dust, are excellent tracers of the underlying stellar mass distribution, because both relatively cool, long-lived, low mass stars—which comprise the bulk of the stellar mass—and old, highly evolved giant stars—whose current distribution has been determined by the gravitational potential of the galaxy—radiate predominantly in the infrared.

Figure 6 is composed of a pair of prints, spanning differing ranges of intensity, produced from a 2.2-μm infrared image of NGC 1068 (*17*). The print on the right exhibits spiral structure in the galaxy similar to that seen in optical photographs. The print on the left reveals a clear stellar bar, with stubby spiral arms emanating from either end. These arms join perfectly onto molecular arm features discovered in radio interferometric observations (*18*), providing stimulating support for the notion of stellar bars as triggers for circumnuclear mass transport and star formation.

On the other hand, NGC 253, a nearby starburst galaxy which seemed from optical and earlier infrared scanning measurements (*19*) to lend additional support to this theory of stellar bars, gives a different impression when imaged in the infrared. Figure 7 is made from optical and infrared pictures of NGC 253. The optical picture is obviously heavily affected by dust. The infrared picture, although confirming the existence of the elongated structure found in the earlier work, shows that the "bar" bends, and must be at least in part a spiral arm. Furthermore, there is no barlike distortion of the brightness distribution approaching the starburst nucleus. An infrared survey of barred spiral galaxies will surely help clarify the role of stellar bars, if any, in transporting "fuel" inward toward the nuclei of galaxies. The color infrared picture here is displayed in "false color": the different colors correspond to differing levels of intensity

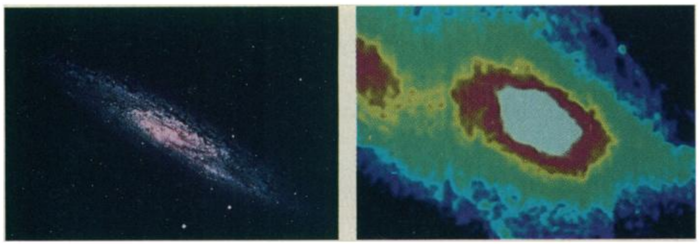

Fig. 7. Comparison of optical and infrared images of NGC 253. (**Left**) A color optical picture, reprinted with permission of the Anglo-Australian Telescope Board. (**Right**) A false color 2.2-μm infrared picture of NGC 253 taken at the Steward Observatory of the University of Arizona with the 61" telescope, courtesy of G. Rieke and M. Rieke. The scales are not the same.

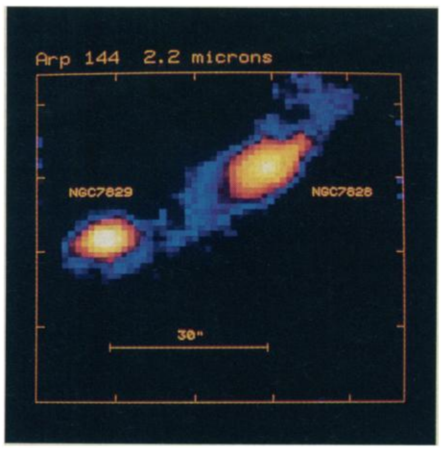

Fig. 8. A false color 2.2-μm infrared image of Arp 144 taken with the University of Texas McDonald Observatory 2.7-m telescope, courtesy of M. Joy and P. Harvey.

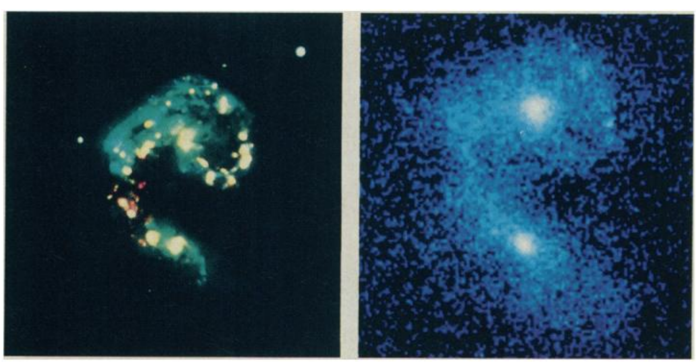

Fig. 9. Comparison of an archival KPNO optical picture (**left**) and a 1.65-μm infrared image (**right**), both in false color, of NGC 4038 and NGC 4039 taken with the Kitt Peak National Observatory 2.1-m telescope. The scales are not the same.

(brightness) for radiation at a single wavelength, rather than radiation at different wavelengths.

Galaxies in Collision

Stars form in molecular clouds, and external triggers (such as the action of the stellar bar in NGC 1068) may stimulate and enhance the process. Perhaps the ultimate example of a trigger is the collision of two galaxies. As well as causing star formation, such a collision would very probably deposit material onto the galactic nuclei, "force-feeding" the accretion disk of a black hole, if one were present. These are plausibly the reasons why the IRAS satellite found interacting galaxies as a class to be the most luminous systems in the universe. The interaction stirs up the interstellar material in the galaxies, causing severe, clumpy extinction. This extinction and the bright emission from regions of induced star formation conspire to produce a chaotic appearance in optical photographs. The large variety of possible outcomes from galaxy/galaxy interactions is briefly illustrated by three examples.

Optical studies of the galaxy Arp 144 (NGC 7828/29) revealed a seemingly empty "folded ring" (NGC 7828) with a spheroidal companion (NGC 7829); this unusual structure was believed to be a spiral galaxy whose disk had been stripped away in a collision with an (invisible) intergalactic cloud of atomic hydrogen (*20*). The infrared image in Fig. 8 shows that Arp 144 was actually formed by an encounter between two similarly massive galaxies (*21*). The extinction within the ring of NGC 7828 is very high, and hides the nucleus at optical wavelengths.

A second interaction is illustrated in Fig. 9, which is composed of the optical and infrared images of the NGC 4038/4039 system. The optical image is dramatically disturbed, speckled with bright centers of star formation, and mottled with dark patches of dust. It is difficult to distinguish the nuclei of the two colliding galaxies. The infrared image is much less chaotic, penetrates through the dust, and shows the distribution of stellar mass in the galaxies rather well.

It has proved difficult to classify interacting galaxies from optical photographs because of the wide variety in their appearance, which has been illustrated, for example, in Arp's *Atlas of Peculiar Galaxies* (*22*). Interacting galaxies are valuable "test particles" for various theoretical formalisms, and infrared images can provide a clear picture of the underlying stellar mass distributions. The possibility exists that classification may be more tractable from infrared images; an infrared survey of interacting galaxies is now feasible. Possibly the components will prove recognizable within the classification scheme used for undisturbed galaxies, in which case we can make a major step, and identify the types of galaxies that collided.

The impact of the technological revolution reported here may be seen in images of even very familiar systems; Fig. 10, for example, is composed of optical and infrared images of the famous "Whirlpool" galaxy (Messier 51). This galaxy was the first in which spiral structure was recognized, in 1845.

The arms of the large spiral appear much more regular in the infrared picture than in the optical. The outlying arm, which joins to the companion, is strikingly faint in the infrared, suggesting that much of its optical luminosity is from young stars formed in the galaxy/galaxy interaction. The companion galaxy is clearly shown by the infrared image to be a barred spiral.

The Detectors

The majority of infrared arrays available today are hybrid devices, resulting from a process in which the detectors and readouts are manufactured separately. The readout circuit is fabricated on silicon in the same way as integrated circuits, whereas the detectors are made, for example, from mercury cadmium telluride (HgCdTe), indium antimonide (InSb), platinum silicide (PtSi), or extrinsic doped silicon (Si:X). Then the two chips are sandwiched together, with the electrical interconnections being made by indium bumps on each of the chips [see (*3*) for details of the construction]. Most of the arrays in use at telescopes today were obtained through collaborations with industry, NASA, or the Department of Defense.

The images included in this article were made with four different types of detector arrays, by observers at a number of institutions, as described in the next paragraph. These arrays share the property that each consists of thousands of detector elements, and that each element of the array outperforms the single detectors of earlier experiments. Briefly, these devices are:

Fig. 10. Comparison of an archival KPNO optical picture (left) and a 1.65-μm infrared picture (right) of M 51. The infrared picture was taken with the Kitt Peak National Observatory 1.3-m telescope. The scales are not the same.

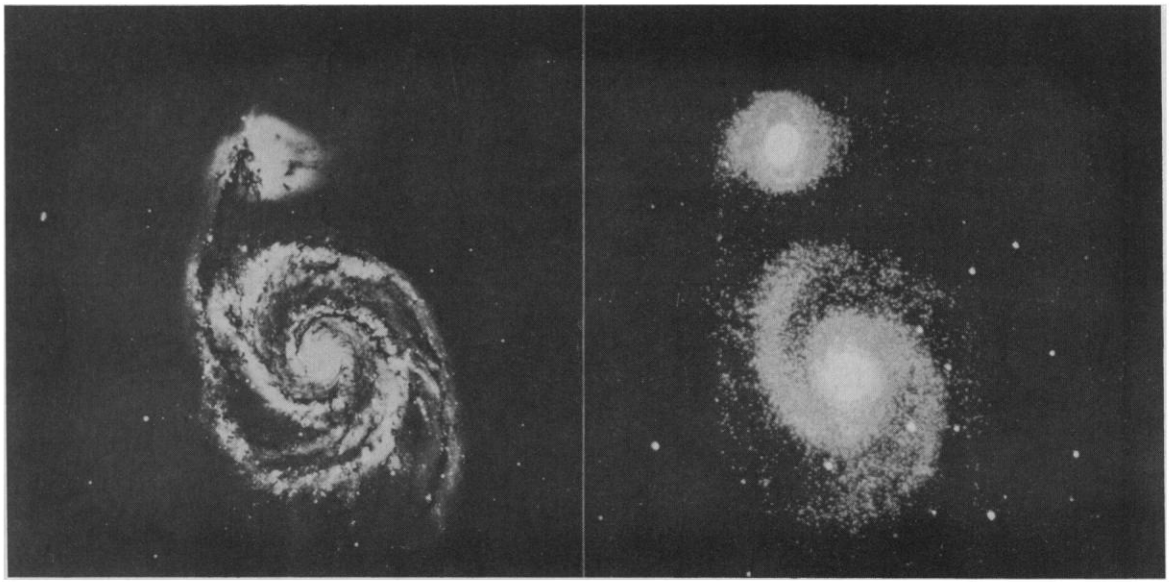

1) A 128 by 128 HgCdTe array with a Reticon metal-oxide semiconductor field effect transistor (MOSFET) multiplexer readout, manufactured by Rockwell Science Center for the Jet Propulsion Laboratory (JPL/HIRIS) and operated by the University of Hawaii (see Fig. 2).

2) A 64 by 64 HgCdTe array with a direct-injection input surface-channel charge-coupled device (CCD) readout manufactured by Rockwell Science Center, and operated both by the University of Arizona and the Astrophysics Research Consortium (ARC) (see Figs. 6 and 7).

3) A 58 by 62 InSb array with a source follower input MOSFET multiplexer readout manufactured by Santa Barbara Research Center, and operated by the University of Texas at Austin, the United Kingdom Infrared Telescope (UKIRT), and the National Optical Astronomy Observatories (NOAO) (see Figs. 1, 3, 4, and 8).

4) A 256 by 256 platinum silicide Schottky barrier diode array with a source follower input MOSFET multiplexer readout, manufactured by Hughes Aircraft Co., and operated by the Infrared Research and Development Group of the National Optical Astronomy Observatory (NOAO/IR&D) (see Figs. 5, 9, and 10 and the cover of this issue).

The HgCdTe array from Rockwell Science Center and the InSb array from Santa Barbara Research Center are available commercially.

Future Prospects

The examples presented here demonstrate the utility and viability of infrared imaging as a tool in astronomy, but rapid improvements in the technology will continue for some time yet. The detector arrays we have described here were an outgrowth of the technology developed by the defense industry for military applications. Feedback to the manufacturers following their first use for astronomy has meant that more recent arrays are being optimized for use in astronomy by improvement in noise and dark-current performance, by modification of the wavelength response, and by changes in readout designs. The number of detector elements in the arrays will continue to be increased, and formats as large as 256 by 256 will be in widespread use within 2 or 3 years.

Although we have concentrated here on the wavelength interval 1 to 2.5 μm, the same principles of array construction are applicable out to wavelengths at least as long as 30 μm, and the same intrinsically high detector sensitivities can be achieved. The realization of the full potential of the arrays at these longer wavelengths is more difficult however, because of the large thermal backgrounds emitted by the atmosphere and the telescopes themselves; a number of groups are already using arrays at longer wavelengths, and there is rapid progress in learning how to cope with the thermal background.

Further strides can be made with array detectors in space, where the thermal background can be eliminated by cooling the telescope; the gains achieved by IRAS were possible because of its cooled telescope (*23*), but this telescope did not have the benefit of arrays. The European Space Agency's Infrared Space Observatory (ISO) will combine a cold telescope with some use of arrays, and both features will be fully exploited by NASA's Space Infrared Telescope Facility (SIRTF) (*24*). NASA is also planning to reach the full resolution available with the Hubble Space Telescope (HST) by outfitting it with a second generation instrument equipped with infrared arrays.

REFERENCES AND NOTES

1. J. F. Arens *et al.*, *Proc. Soc. Photo. Opt. Instrum. Engin.* **280**, 61 (1981).
2. W. J. Forrest and J. L. Pipher, in *Proceedings of the Infrared Detector Technology Workshop*, C. R. McCreight, Ed. (U.S. Government Printing Office, Washington, DC, 1983), pp. 161–169.
3. C. G. Wynn-Williams and E. E. Becklin, Eds., *Infrared Astronomy with Arrays* (University of Hawaii, Institute for Astronomy, Honolulu, 1987).
4. G. L. Grasdalen, *Astrophys. J.* **193**, 373 (1974).
5. E. Krugel, C. Thum, J. Martin-Pintado, H. Pankonin, *Astron. Astrophys. Suppl. Ser.* **48**, 345 (1982).
6. B. G. Elmegreen, C. J. Lada, D. F. Dickinson, *Astrophys. J.* **230**, 425 (1979).
7. D. A. Harper, F. J. Low, G. H. Rieke, H. A. Thronson, *ibid.* **205**, 136 (1976).
8. R. L. Snell, in *Star Forming Regions, Proceedings of the 115th IAU*, M. Peimbert and J. Jugaku, Eds. (Reidel, Dordrecht, 1985), pp. 213–237.
9. I. Gatley, in *Galactic and Extragalactic Star Formation, NATO Advanced Study Institute*, G. Fick and R. Pudritz, Eds. (Reidel, Dordrecht, 1988), pp. 159–179.
10. J. H. Black and E. F. van Dishoeck, *Astrophys. J.* **322**, 412 (1987).
11. B. Zuckerman and I. Gatley, *ibid.* **324**, 1222 (1988).
12. E. E. Becklin and G. Neugebauer, *ibid.* **151**, 145 (1968).
13. D. C. Backer, Ed. *The Galactic Center: Proceedings of the Symposium Honoring C. H. Townes* (American Institute of Physics, New York, 1987).
14. C. M. Telesco, E. E. Becklin, C. G. Wynn-Williams, D. A. Harper, *Astrophys. J.* **282**, 427 (1984).
15. H. J. Habing and G. Neugebauer, *Sci. Am.* **251**, 49 (November 1984).
16. T. G. Hawarden, J. H. Fariclough, R. D. Joseph, S. K. Leggett, in *Light on Dark Matter*, F. P. Israel, Ed. (Reidel, Dordrecht, 1985), pp. 455–466.
17. H. A. Thronson *et al.*, *Astrophys. J.*, in press.
18. S. T. Meyers and N. Z. Scoville, *ibid.* **312**, L39 (1987).

19. N. Z. Scoville *et al.*, *ibid.* **289**, 129 (1985).
20. K. C. Freeman and G. de Vaucouleurs, *ibid.* **194**, 569 (1974).
21. M. Joy *et al.*, *ibid.* **330**, L29 (1988).
22. H. Arp, *Atlas of Peculiar Galaxies* (California Institute of Technology, Pasadena, 1966).
23. G. Neugebauer *et al.*, *Science* **224**, 14 (1984).
24. G. H. Rieke *et al.*, *ibid.* **231**, 807 (1986).
25. This article reports the success of the community of people who do infrared astronomy: we are especially grateful to J. Arens, E. Anderson, B. Balick, J. Barnes, P. Britt, N. Buchholz, G. Burbidge, E. Becklin, L. Davis, W. Forrest, M. Fowler, S. Gaalema, J. Gates, Cathy and Sam Gatley, F. Gillett, K. Gillies, M. Hanna, A. Harper, P. Harvey, M. Hereld, K. Hodapp, M. Joy, R. Joyce, C. Lada, J. Little, I. McLean, M. Merrill, J. Pipher, R. Probst, G. Rieke, M. Rieke, F. Stuart, H. Thronson, S. Wolff, and B. Zuckerman. The National Optical Astronomy Observatories are operated by the Association of Universities for Research in Astronomy, Inc., under contract with the National Science Foundation.

Research Articles

RNA Processing Generates the Mature 3′ End of Yeast *CYC1* Messenger RNA in Vitro

J. SCOTT BUTLER AND TERRY PLATT

In whole cell extracts of *Saccharomyces cerevisiae*, incubation of precursor mRNA transcripts encoding the sequences essential in vivo for forming the 3′ end of the iso-1-cytochrome c mRNA (*CYC1*) revealed an endonuclease activity with the characteristics required for producing the mature mRNA 3′ end. The observed cleavage in vitro is (i) accurate, occurring at or near the polyadenylation site of *CYC1* RNA, (ii) 30 to 50 percent efficient, (iii) adenosine triphosphate dependent, (iv) specific for the 3′ ends of at least two yeast pre-mRNA's, and (v) absent with related pre-mRNA's carrying mutations that abolish correct 3′ end formation in vivo. In addition, a second activity in the extract polyadenylates the product under appropriate conditions. Thus, the mature 3′ ends of yeast mRNA's may be generated by endonucleolytic cleavage and polyadenylation rather than by transcription termination.

IN EUKARYOTIC CELLS, MESSENGER RNA'S REQUIRE POST-transcriptional modification before export from the nucleus to the cytoplasm. These modifications include capping of the 5′ terminus, methylation of some internal adenosines, and RNA splicing to remove internal noncoding introns and then join the separated exons into a contiguous mRNA. In higher eukaryotes, the formation of the mature 3′ end of mRNA's also requires RNA processing which entails (except for most of the histone transcripts) endonucleolytic cleavage and polyadenylation of a primary transcript, or pre-mRNA, that extends some distance beyond the mature 3′ end of the message (*1*). The extent of gene expression depends on (i) efficient polyadenylation of mRNA's to enhance the stability of the message (*2*) and (ii) selection of the correct polyadenylation site to produce the desired protein product. For example, some human thalassemias result from mutations in the conserved AAUAAA polyadenylation signal that abolish correct 3′ end formation and thus reduce globin gene expression in the affected individuals (*3, 4*). Where alternative polyadenylation signals exist, selection among them provides a mechanism to control gene expression. In developing B cells, the shift from one polyadenylation signal to another causes a change in the production of immunoglobulin M heavy chain from the membrane bound to the secreted form (*5*), and selection of polyadenylation sites affects the relative amounts of adenovirus mRNA's during infection (*6, 7*). These examples reveal the widespread involvement of mechanisms determining mRNA 3′ end formation in the regulation of gene expression.

In higher eukaryotes, cleavage and polyadenylation require the nucleotide signal AAUAAA, which is about 20 nucleotides 5′ to the cleavage site (*8, 9*), as well as some less conserved GU- or U-rich sequences just distal to the polyadenylation site (*10–13*). In *Saccharomyces cerevisiae*, however, all known RNA polymerase II transcripts (including the histone mRNA's as well as aberrant mRNA's) become polyadenylated after synthesis, yet known sequences of yeast mRNA's do not share an AAUAAA signal or any other highly conserved sequence identified as responsible for 3′ end formation. Zaret and Sherman discovered that a mutation (*cyc1-512*) deleting 38 base pairs 3′ to the coding sequence of the iso-1-cytochrome *c* gene (*CYC1*) causes a 90 percent decrease in the amount of *CYC1* mRNA (*14*). The residual mRNA's produced are all longer than normal and they are all polyadenylated, suggesting that some crucial elements of the normal 3′ end formation signal are deleted. Comparison of sequences from the *cyc1-512* deletion with those from other DNA fragments that apparently direct mRNA 3′ end formation in yeast (*15–18*) shows similarities, but none of the proposed consensus sequences fit all of the known 3′ end regions. This lack of strong sequence similarity and the fact that all RNA polymerase II transcripts are polyadenylated led to the suggestion that polyadenylation might be coupled to transcription termination (*14*) and that a protein factor analogous to *Escherichia coli* transcription termination factor rho might be involved in mRNA 3′ end formation in yeast (*16*).

These considerations and the recent discovery that *E. coli* rho factor catalyzes the unwinding of RNA-DNA helices (*19*) led us to search for a rho-type helicase activity in yeast whole cell extracts. In the course of this search we discovered that *CYC1* pre-mRNA sequences are accurately cleaved and polyadenylated in vitro. The formation of 3′ ends of yeast mRNA's may thus be independent of transcription termination, and our results suggest that yeast process

The authors are at the Department of Biochemistry, University of Rochester Medical Center, 601 Elmwood Avenue, Rochester, NY 14642.